

Topological Superconductivity and Majorana Fermions in RKKY Systems

Jelena Klinovaja,¹ Peter Stano,^{1,2} Ali Yazdani,³ and Daniel Loss¹

¹*Department of Physics, University of Basel, Klingelbergstrasse 82, CH-4056 Basel, Switzerland*

²*Institute of Physics, Slovak Academy of Sciences, 845 11 Bratislava, Slovakia*

³*Joseph Henry Laboratories and Department of Physics,*

Princeton University, Princeton, New Jersey 08544

(Dated: July 22, 2013)

We consider quasi one-dimensional RKKY systems in proximity to an s -wave superconductor. We show that a $2k_F$ -peak in the spin susceptibility of the superconductor in the one-dimensional limit supports helical order of localized magnetic moments via RKKY interaction, where k_F is the Fermi wavevector. The magnetic helix is equivalent to a uniform magnetic field and very strong spin-orbit interaction (SOI) with an effective SOI length $1/2k_F$. We find the conditions to establish such a magnetic state in atomic chains and semiconducting nanowires with magnetic atoms or nuclear spins. Generically, these systems are in a topological phase with Majorana fermions. The inherent self-tuning of the helix to $2k_F$ eliminates the need to tune the chemical potential.

PACS numbers: 75.75.-c, 74.20.-z, 75.70.Tj, 73.63.Nm

Introduction. Majorana Fermions (MFs)¹ have attracted wide attention due to their exotic non-Abelian statistics and their promise for topological quantum computing,^{2,3} also fueled by recent experiments searching for MFs.⁴⁻¹⁰ The crucial ingredient for most MF proposals are helical spin textures leading to an exotic p -wave pairing due to proximity effect with an ordinary s -wave superconductor.^{3,11-14} The associated helical modes, which transport opposite spins in opposite directions, are proposed to exist in various systems.¹³⁻²¹ A well-known mechanism responsible for helical modes is spin-orbit interaction (SOI) of Rashba type.^{3,11,12} However, quite often, an additional uniform magnetic field is needed, and the spin polarization of the helical modes is not ideal but depends on the SOI strength¹⁵. While intrinsic values of SOI are limited by material parameters, the recently proposed synthetic SOI produced by a helical magnetic field can reach extraordinary values that are limited only by the spatial period of the helical field $2\pi/k_n$.²² Such helical fields can be engineered with nanomagnets,²⁰⁻²⁵ or, more atomistically, can emerge from helical spin chains due to anisotropic exchange and Dzyaloshinskii-Moriya interaction.²⁶⁻²⁹ The equivalence between spectra of wires with intrinsic and with synthetic SOI has opened up new platforms for helical modes and MFs.²⁰⁻²⁴ However, in all these setups the chemical potential must be tuned inside the gap opened by the magnetic field so that the Fermi wavevector k_F is close to $k_n/2$. This poses additional challenges on experimental realizations by requiring wires with a high tunability of the Fermi level and high mobility down to ultra-low densities.

Thus, it is natural to ask if helical modes exist in low-dimensional superconductors such that the system automatically tunes itself to $k_n = 2k_F$. Surprisingly, the answer turns out to be affirmative for a rather broad class of systems. These are RKKY systems that consist of localized magnetic moments coupled by itinerant electrons via the Rudermann-Kittel-Kasuya-Yosida (RKKY)

interaction.³⁰⁻³² It was recently discovered that in such systems in the quasi one-dimensional (1D) limit the moments form a spin helix leading to a Peierls-like gap at the intrinsic Fermi level such that $2k_F = k_n$.^{22,33-35} However, these results were obtained for semiconducting or metallic systems in the normal phase, relying on the presence of gapless itinerant electrons to transmit the RKKY interaction. Thus, it is not clear that the same ordering mechanism can also develop in the superconducting regime where the spectrum of the electrons is gapped. In the present Letter we address this issue in detail and demonstrate that the helical order arising from RKKY interaction survives also in 1D superconductors. As a prototype for our model we consider atomic chains²⁶ and semiconducting nanowires with magnetic atoms or nuclear spins placed on top of a bulk s -wave superconductor. We show that these setups are generically deep inside the topological phase and host MFs without requiring any fine-tuning at all.

Model. We consider a quasi 1D superconducting wire aligned along the x -axis with embedded localized magnetic moments, see Fig. 1. The quasi-one-dimensionality means that only the lowest subband of the wire is occupied,³⁶ and the wavefunction in the transverse direction is given by $\psi(y, z) \equiv \psi(\mathbf{r}_\perp)$. The 1D s -wave su-

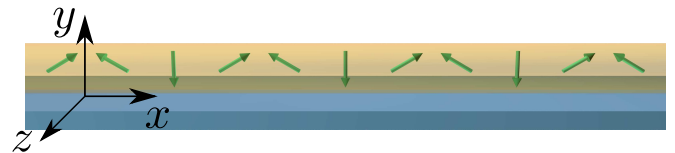


FIG. 1. Sketch of a wire (yellow cylinder) aligned along the x -axis brought into contact with an s -wave superconductor (blue slab). Localized magnetic moments (green arrows) are ordered into a spin helix by RKKY interaction transmitted by electrons.

perconductor is described by the Hamiltonian

$$H = \int dx [\psi^\dagger \mathcal{H}_0(x) \psi + \Delta_s (\psi_\uparrow \psi_\downarrow + \text{h.c.})], \quad (1)$$

where $\psi(x) = (\psi_\uparrow(x), \psi_\downarrow(x))$ with $\psi_\sigma(x)$ being an annihilation operator acting on an electron at position x with spin σ . The superconducting coupling parameter $\Delta_s \geq 0$ arises from the proximity effect. Here, $\mathcal{H}_0(x) = -\hbar^2 \partial_x^2 / 2m - \mu_F$, where m is the effective mass and $\hbar \hat{k} = -i\hbar \partial_x$ the momentum operator. The energy is taken from the Fermi level, $\epsilon_k = \hbar^2(k^2 - k_F^2)/2m$, where the Fermi wavevector $k_F = \sqrt{2m\mu_F}/\hbar$ is set by the chemical potential μ_F . The quasiparticle energy in the superconductor is given by $\eta_k = \sqrt{\epsilon_k^2 + \Delta_s^2}$.

The interaction between itinerant electron spins and localized magnetic moments $\tilde{\mathbf{I}}_i$ at position $\mathbf{R}_i = (x_i, \mathbf{r}_{\perp,i})$ is described by the Hamiltonian density

$$\mathcal{H}_{int}(x) = \frac{\beta}{2} \sum_i \tilde{\mathbf{I}}_i \cdot \boldsymbol{\sigma} |\psi(\mathbf{r}_{\perp,i})|^2 \delta(x - x_i), \quad (2)$$

with the coupling strength β being a material constant. Here, $\boldsymbol{\sigma}$ is the vector of Pauli matrices acting in electron spin space. In the following we solve the interacting Hamiltonian $H + H_{int}$ on a mean field level: We first integrate out the superconducting condensate in leading order β to derive an effective RKKY interaction for the subsystem of localized moments. We find its groundstate and quantify conditions under which it is stable. Assuming these conditions are fulfilled, we derive an effective Hamiltonian for the electron subsystem.

RKKY in a 1D superconductor. The localized moments spin-polarize the conducting medium, which influences other moments and results in the RKKY interaction. We now introduce an effective 1D model of magnetic moments, with a notation suitable for magnetically doped semiconductor wires, and extend it later to other realizations. We approximate the transverse wavefunction profile $|\psi(\mathbf{r}_{\perp})|^2$ by a constant, the inverse of the cross-section area A . We assume there are N_{\perp} localized moments on a transverse plane. Though N_{\perp} might be large, once the magnetic order is established, these spins are collinear, since the spin excitations within the locked transverse plane are energetically much more costly than excitations we will consider below and can therefore be neglected.³³ Thus, a transverse plane is assigned a single (effective) spin of length $I = N_{\perp} \tilde{I}$. Neighboring planes are separated by a distance of the order of the lattice constant a , and the density of moments is parametrized as $N_{\perp} = \alpha \rho_0 A a$, with α being the fraction of cations replaced by magnetic atoms and $\rho_0 = 4/a^3$ the cation density in zinc-blende materials.

With these definitions, the RKKY interaction between localized moments becomes

$$H^{RKKY} = - \sum_{i,j} J_{ij} \mathbf{I}_i \cdot \mathbf{I}_j, \quad (3)$$

where the long range coupling $J_{ij} = -\frac{2\beta^2}{A^2} \chi(x_i - x_j)$ is given by the static spin susceptibility χ of

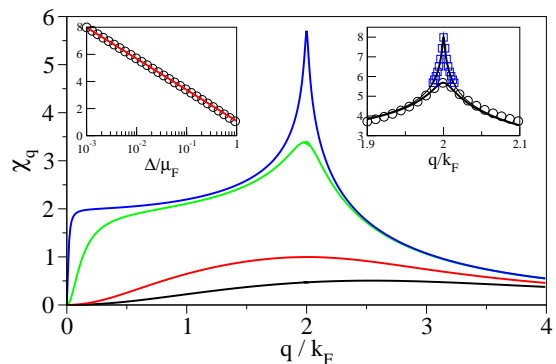


FIG. 2. (Color online) One-dimensional superconductor susceptibility divided by $k_F/8\pi a\mu_F$. Main: Susceptibility given in Eq. (4) for $\Delta_s/\mu_F = 2, 1, 0.1$, and 0.01 , *resp.* (curves from bottom up). Insets: comparison of exact [symbols; Eq. (4)] and interpolation [solid line; Eq. (5)] values. Left: at $q = 2k_F$. Right: for $\Delta_s/\mu_F = 0.01$ (circles), and 0.001 (squares).

the 1D superconductor. In Fourier space, $\chi_q = (1/a) \int dx \exp(iqx) \chi(x)$, the susceptibility at zero temperature is given by³⁸

$$\chi_q = -\frac{1}{4aL} \sum_k \frac{\eta_k \eta_{k+q} - \epsilon_k \epsilon_{k+q} - \Delta_s^2}{\eta_k \eta_{k+q}} \frac{1}{\eta_k + \eta_{k+q}}. \quad (4)$$

Here, $L = Na$ is the system length. The finite temperature corrections to χ , being exponentially small if $\Delta_s \gg k_B T$, are neglected. For a plot of χ_q , see Fig. 2.

Though $\chi_{q=0} = 0$ and thus the total magnetization is strictly zero,³⁹ the superconductor responds at non-zero momenta q . If $\Delta_s \leq \mu_F$, the susceptibility develops a peak at $q = 2k_F$, which gets more pronounced as the ratio Δ_s/μ_F drops. Examining the limiting cases analytically, we suggest the following interpolation formula

$$\chi_q \approx -\frac{k_F}{8\pi a\mu_F} \ln \left(\frac{e^{1/2+\gamma}}{\sqrt{\Delta_s^2/\mu_F^2 + (1 - q/2k_F)^2/2}} \right), \quad (5)$$

in the regime of $\Delta_s \lesssim \mu_F$ and $|q - 2k_F| \ll k_F$. Here, $\gamma \approx 0.58$ is the Euler gamma constant. Comparing to numerics, we find that it is an excellent approximation for the peak height at $q = 2k_F$, while away from this point it differs from the exact result by a broad non-resonant background only (see insets of Fig. 2).

Magnons. The classical ground state of Eq. (3) with J peaked at finite momentum is a helically ordered pattern, $\mathbf{I}_i = \mathcal{R}_{\mathbf{h}, 2k_F x_i} [\mathcal{I}]$ with \mathcal{R} a 3×3 matrix corresponding to a vector rotation around the helical axis \mathbf{h} and angle $2k_F x_i$, and $\mathcal{I} \equiv \mathbf{I}_1 \perp \mathbf{h}$ is the spin at the wire end. We find the excitations of the corresponding quantum system (magnons) by Holstein-Primakoff representation of the effective spins by bosons.⁴⁰ Magnons, labelled by momentum k , have energies

$$\hbar\omega_k = \frac{\tilde{I}}{\sqrt{2}} \sqrt{\left(2J_{2k_F}^{\parallel} - J_{2k_F+k}^{\parallel} - J_{2k_F-k}^{\parallel} \right) \left(J_{2k_F}^{\parallel} - J_k^{\perp} \right)}, \quad (6)$$

	chain	magnetic wire	nuclear wire
material	Fe	GaMnAs	InAs
a	0.3 nm	0.565 nm	0.605 nm
g_e	2	-0.44	-8
$\tilde{I} \cdot g_s \cdot \mu$	$2 \cdot 2 \cdot \mu_B$	$5/2 \cdot 2 \cdot \mu_B$	$9/2 \cdot 1.2 \cdot \mu_N$
β	1.6 meV nm ³	9 meV nm ³	4.7 μ eV nm ³
α	1	0.02	1
μ_F	10 meV	20 meV	1 meV
Δ_s	1 meV	0.5 meV	0.1 meV
T_c	14 K	2 K	7.4 mK
B_c	5 T	0.7 T	0.4 T
Δ_m	6 meV	5 meV	0.2 meV
ξ	4 nm	0.4 μ m	0.5 μ m

TABLE I. Chosen parameter values: material, lattice constant a , electron g -factor g_e , magnetic moment $\mu_S = \tilde{I}g_s\mu$, exchange coupling β , moment doping α , Fermi energy μ_F , superconducting gap Δ_s , and the resulting scales: critical temperature T_c , critical field B_c , effective helical field strength Δ_m , and MF localization length ξ for different realizations: magnetic atom chain, magnetically doped nanowire, and nanowire with nuclear spins. The effective mass for GaMnAs (InAs) is $m = 0.067m_e$ ($0.027m_e$).

where we introduced the upper index on the tensor J for its value in the helical plane (\parallel) and in a direction perpendicular to it (\perp). We consider first the isotropic case, $J_q^\parallel = J_q^\perp$. The spectrum is gapless, as the two terms under the square root in Eq. (6) become zero at $k = 0$ and $k = 2k_F$, respectively. Close to these values the dispersion is linear in k , as the function J has a maximum at $2k_F$. The helical order critical temperature follows as (for details see App. B)

$$k_B T_c \sim I^2 J_{2k_F} = -\langle H^{RKKY} \rangle / N \equiv E_h, \quad (7)$$

so that it is given by the RKKY energy scale with expectation value taken in the helical ground state. The critical length turns out to be extremely long and of no concern (see App. B).

Realizations. Next, we discuss three realizations of our system: magnetically doped semiconductor nanowire, such as GaMnAs, clean III-V semiconductor nanowire with high nuclear spin isotopes, such as InAs, and a chain of magnetic atoms on a superconductor surface, such as Fe on Nb. The parameters and resulting scales are summarized in Tab. I. We include the effective field $\Delta_m = \alpha\beta\rho_0\tilde{I}/2$ the electrons feel once the order is established, and $B_c = \min\{E_h/\mu_S, \Delta_m/g_e\mu_B\}$ gives a rough estimate of the critical field B_c destroying the helical order.

For a semiconductor nanowire with a moderate doping of 2% we obtain a critical temperature of Kelvins and stability with respect to magnetic fields in the range of Tesla. Such nanowires can be grown very clean, with mean free paths of order microns if undoped, and are tunable by gates. Magnetic dopants will unavoidably in-

duce some disorder. This problem is absent in the case of an undoped wire with nuclear spins, though there the critical temperature becomes very small, 7 mK, because of the weak hyperfine interaction. We still include this realization for comparison, as establishing helical order in a nuclear wire was considered for electrons in a Luttinger liquid regime.^{33,34} Like there, we expect interactions (neglected here) to enhance T_c by a factor of 2-4. We took InAs as the nuclear wire material and, to simplify notation in Tab. I, we neglected the contribution of As nuclei, thus $\alpha = 1$.

An exciting possibility is offered by magnetic monoatomic chains which can be fabricated on metal²⁶ or superconducting surfaces using either growth or atomic manipulation techniques with the STM.^{28,41} For the latter system, the formulas we give are valid upon putting $N_\perp = 1$, $\alpha = 1$, $A = a^2$ with a being the interatomic distance. As an estimate, we take $\beta/a^3 = 6$ meV and a hopping matrix element $t = 10$ meV.^{26,28,41} The stability of the helical order is rather high, comparable to the stability of the underlying superconductor, so that possible differences in these parameters are not relevant for us. What is important here is that the atomistic exchange and possible spin-orbit based Dzyaloshinskii-Moriya interaction should be negligible for the RKKY-induced magnetism. Under this condition, the magnetic helix pinned to the Fermi level is to be expected.

Majorana Fermions without tuning. From now on we consider a helical order of localized magnetic moments to be established. These moments $\tilde{\mathbf{I}}_i$ are aligned along the polarization vector $\mathbf{n}(x) = \cos(2k_F x)\hat{x} + \sin(2k_F x)\hat{y}$, that is perpendicular to the helix-axis $\mathbf{h} \equiv \hat{z}$. Such an ordered state acts back on the electrons via $\mathcal{H}_{int}(x)$ [see Eq. (2)] that takes the form of an effective Zeeman term

$$\mathcal{H}_m = \Delta_m \mathbf{n}(x) \cdot \boldsymbol{\sigma}, \quad (8)$$

where $\Delta_m = \alpha\beta\rho_0\tilde{I}/2$ is the strength of the helical field assumed to be positive from now on.

The energy spectrum of a system described by $\mathcal{H} + \mathcal{H}_m$ can be easily found by rewriting all electron operators in terms of slow-varying right- (R_σ) and left- (L_σ) movers: $\psi_\sigma(x) = R_\sigma(x)e^{ik_F x} + L_\sigma(x)e^{-ik_F x}$.⁴² The helical field with a pitch π/k_F results in a resonant scattering between right movers with spin down and left movers with spin up, see Fig. 3a. Taking this resonance into account, we arrive at the effective Hamiltonian $\tilde{H} = \frac{1}{2} \int dx \phi^\dagger(x) \mathcal{H} \phi(x)$ with the Hamiltonian density

$$\tilde{\mathcal{H}} = -i\hbar v_F \tau_3 \partial_x + \frac{\Delta_m}{2} \eta_3 (\sigma_1 \tau_1 + \sigma_2 \tau_2) + \Delta_s \eta_2 \sigma_2 \tau_1, \quad (9)$$

where the Pauli matrix τ_i (η_i) acts in left-right mover (electron-hole) space, and $\phi = (R_\uparrow, L_\uparrow, R_\downarrow, L_\downarrow, R_\uparrow^\dagger, L_\uparrow^\dagger, R_\downarrow^\dagger, L_\downarrow^\dagger)$. The Fermi velocity is given by $\hbar v_F = (\partial \epsilon_k / \partial k)|_{k=k_F}$. The diagonalization

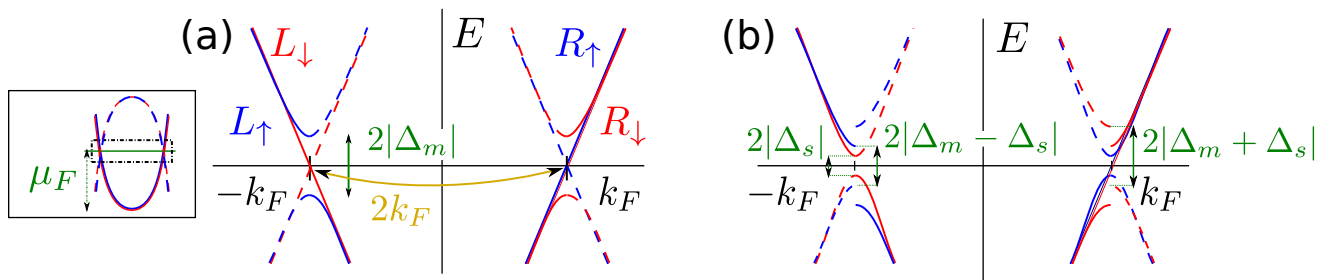


FIG. 3. (a) Electron (solid lines) and hole (dashed lines) energy spectrum around the Fermi points $\pm k_F$ of a wire in the presence of a helical magnetic field described by $\mathcal{H}_0 + \mathcal{H}_m$. The inset shows the entire spectrum of \mathcal{H}_0 with μ_F being counted from the band bottom. The interaction term \mathcal{H}_m leads to a resonant scattering between right movers with spin down R_\downarrow and left movers with spin up L_\uparrow and results in a partial gap $2\Delta_m$ in the spectrum. Away from the Fermi points spin up (blue lines) and spin down (red lines) states stay degenerate. (b) The superconducting pairing term of strength Δ_s , which couples electron-hole states with opposite spins and momenta, gaps all branches of the spectrum [see Eqs. (10)-(11)] except for the special case $\Delta_s = \Delta_m$, which marks the transition between trivial and topological phases.

of $\tilde{\mathcal{H}}$ gives us the bulk spectrum,

$$E_{\pm}^{(1)} = \pm \sqrt{(\hbar v_F k)^2 + \Delta_s^2}, \quad (10)$$

$$E_{\pm}^{(2,\pm)} = \pm \sqrt{(\hbar v_F k)^2 + (\Delta_m \pm \Delta_s)^2}. \quad (11)$$

Here, k is the momentum eigenvalue defined close to the Fermi points $\pm k_F$. The Hamiltonian \mathcal{H} belongs to the topological class BDI⁴³, so the system can potentially host MFs. The transition between a topological phase (with MFs) and a trivial phase (no MFs) is related to closing and reopening of an energy gap. In our case, the system is gapless if $\Delta_m = \Delta_s$, see Eq. (11) for $E_{\pm}^{(2,-)}$. Straightforward calculations^{23,42} lead us to the topological criterion $\Delta_m > \Delta_s$. If it is satisfied, the system is in the topological phase. We note that for all three realizations considered above $\Delta_m \gg \Delta_s$ (see Tab. I), so the system is automatically deeply in the topological phase without any need for parameter tuning.

The MF localization length ξ is determined by the smallest gap in the system, $\xi = \hbar v_F / \Delta_s$. If the distance L between MFs localized at opposite ends of the wire is smaller than ξ , these two MFs combine into an ordinary fermion of non-zero energy.⁴⁴ The numerical values for ξ listed in Tab. I are well below a micrometer. In addition, the coupling between MFs can take place via the bulk superconductor.⁴⁵ However, this channel is also efficiently suppressed in long wires.

We have tested our model numerically. As expected, the presence of MFs in the topological phase is stable against fluctuations of hopping parameters, the superconductivity strength, and the local chemical potential. We believe that disorder effects, which challenge an observation and identification of MFs,^{44,46-51} can be efficiently suppressed in our setup. Unlike to Rashba nanowires, where the charge density is limited by the (usually weak) Rashba SOI, we can work at much higher densities benefitting from charge impurities being screened. However, if μ_F is increased, the critical temperature T_c goes slowly down [as $1/k_F$, see Eq. (7)]. For an atom chain, which can be charged by gates, this is

irrelevant as T_c is very high to begin with. For a semiconducting nanowire, the decrease of T_c can be prevented by increasing magnetic doping.

Conclusions. We have introduced a new class of superconducting systems based on RKKY interactions which feature magnetic helices with a pitch given by half of the Fermi wavelength in the quasi one-dimensional limit. As a result, the superconductor becomes topological and hosts MFs without the need to tune the chemical potential. We have proposed candidate systems such as chains of magnetic atoms and semiconducting nanowires with nuclear spins or magnetic dopants.

ACKNOWLEDGMENTS

We acknowledge support by the SNF, NCCR QSIT, COQI-APVV-0646-10, nsf-dmr1104612, and ARO.

Appendix A: Spin susceptibility

The spin susceptibility, the expression for which we give in the main text, see Eq. (4), is defined by the relation

$$\langle \mathbf{s}(x) \rangle = \int dx' \chi(x-x') \mu \mathbf{B}(x'), \quad (S1)$$

for the expectation value of the spin density $\mathbf{s}(x) = \psi^\dagger(x) (\boldsymbol{\sigma}/2) \psi(x)$ arising in response to a magnetic field perturbation $H_m = - \int dx \mu \mathbf{B}(x) \cdot \mathbf{s}(x)$.

Appendix B: Magnons

First we address the question of the critical temperature and length associated with fluctuations in low dimensions. Magnons are excitations of the helical ground state of localized magnetic moments. Without magnons

the order is perfect—the total spin polarization P is maximal—while each magnon diminishes it by one unit of μ_B . Magnons have Bose-Einstein statistics, and at finite temperature T we get

$$P(T) = NI - \sum_{k \neq 0, 2k_F} \frac{1}{\exp(\hbar\omega_k/k_B T) - 1}, \quad (\text{S2})$$

with the magnon dispersion ω_k given in Eq. (6) in the main text. The two terms with exactly zero energy were excluded from the summation, as these do not diminish the polarization, but rather transform one ground state into another. Namely, if J is isotropic, the ground state has continuous symmetry (the full spin rotational symmetry), which, in our model, translates into the symmetry of rotation of \mathcal{I} (spin polarization vector at the wire end) around \mathbf{h} (the vector defining the helical plane) and the rotation of \mathbf{h} itself. As hinted by Eq. (6) of the main text, these two transformations correspond to the two Goldstone bosons $k = 0$, and $2k_F$, respectively. In the limit $L \rightarrow \infty$ the sum in Eq. (S2) is converted into an integral which necessarily diverges because of vanishingly small energies of magnons in the vicinity of the Goldstone bosons.

From the previous discussion it follows that the order can be established only if the system symmetries are broken, for example, by an anisotropy in the RKKY tensor, $J^{\parallel} \neq J^{\perp}$. Such an anisotropy pins the helical axis to certain relative direction to the wire axis, wire-substrate interface, and crystallographic axes. We expect the difference $J^{\parallel} - J^{\perp}$ to be of the order of J^{\parallel} itself, resulting in the gap $\hbar\omega_{2k_F} \sim SJ_{2k_F}$. Alternatively, an easy axis ($K < 0$) or easy plane ($K > 0$) anisotropy seen by the localized spin $H_i = K(\mathbf{S}_i \cdot \mathbf{n}_a)^2$ with \mathbf{n}_a being some fixed direction, has similar consequences and induces a gap $\hbar\omega_{2k_F} \sim 2S|K|$. Finally, a magnetic field B gives a gap $\hbar\omega_{2k_F} \sim 2\mu_S B$, with μ_S being the magnetic moment of the localized spin.

All these perturbations leave the spectrum at $k = 0$ gapless. This is because it stems from symmetry with respect to translations along the wire (equivalent to rotation of \mathcal{I} around \mathbf{h}), which is not broken by any translationally invariant interaction. This symmetry is broken by finite size effects. Pinning the spins on the wire end(s) by some energy K leads to $k = 0$ magnon energy of order K/N . A finite system length L defines the smallest available magnon wavevector $k_1 = 2\pi/L$. It is to be compared to the width of the susceptibility peak $q_w \equiv 2\pi/L_w$, for which we get from Eq. (5) of the main text the value $L_w = (2\pi/k_F)\sqrt{\mu_F/2\Delta}$. For a wire shorter than L_w

there are no low energy magnons—all available ones have energy of order $\hbar\omega \sim SJ_{2k_F}$. Then we obtain the critical temperature of helical order by approximating the magnon energies in Eq. (S2) by a constant, resulting in Eq. (7) of the main text. We list the cut-off length L_w for the three realizations in Tab. SI.

For a wire longer than L_w , magnons in the vicinity of $k = 0$ get more populated. With a linear spectrum, in the $L \rightarrow \infty$ limit, the critical temperature drops logarithmically with L . However, since the susceptibility peak is very narrow, we find that Eq. (7) holds up to exponentially large lengths with a conservative estimate

$$L \lesssim L_w \exp\left(\frac{L_w}{a}\right), \quad (\text{S3})$$

so that Eq. (7) holds for any reasonable wire length before fluctuations suppress the helical order.

	chain	magnetic wire	nuclear wire
L_w	14 nm	150 nm	500 nm

TABLE II. Cut-off length L_w . There are no low energy magnons for wires shorter than L_w leading to the constraint on the wire length L given in Eq. (S3).

Appendix C: Equivalence to spin-orbit coupling

Let us consider the single-particle Hamiltonian of one-dimensional free electrons under the effect of a rotating magnetic field

$$H = \frac{\hbar^2 \hat{k}^2}{2m} - \mu_F + \mathcal{R}_{\mathbf{h}, 2k_F x}[\mathcal{I}] \cdot \boldsymbol{\sigma}. \quad (\text{S4})$$

We introduce a unitary transformation $\mathcal{H}' = U^\dagger \mathcal{H} U$, corresponding to a basis change $\psi'(x) = U^\dagger \psi(x)$. Choosing $U = \exp(-i\mathbf{h} \cdot \boldsymbol{\sigma} k_F x)$, we get that the previous Hamiltonian is equivalent to one with a static magnetic field and a spin-orbit interaction,²²

$$\mathcal{H}' = \frac{\hbar^2 \hat{k}^2}{2m} - \frac{\hbar^2 \hat{k}}{ml_{\text{so}}} \mathbf{n}_{\text{so}} \cdot \boldsymbol{\sigma} + \mu_B \mathbf{B} \cdot \boldsymbol{\sigma}. \quad (\text{S5})$$

Here, the spin-orbit length is given by $l_{\text{so}} = 1/2k_F$ ($l_{\text{so}} \equiv 1/k_n$). The spin-orbit vector points along the helical axis $\mathbf{n}_{\text{so}} \parallel \mathbf{h}$ and the magnetic field \mathbf{B} of strength $\mu_B B = \Delta_m$ points along \mathcal{I} . Importantly, if the spin quantization axis is chosen along \mathbf{h} , the superconducting terms stay invariant, e.g. $\psi'_\uparrow(x)\psi'_\downarrow(x) = \psi_\uparrow(x)\psi_\downarrow(x)$.

¹ E. Majorana, Nuovo Cimento 14, 171 (1937).

² A. Y. Kitaev, Phys. Usp. 44, 131 (2001).

³ J. Alicea, Rep. Prog. Phys. 75, 076501 (2012).

⁴ S. Sasaki, M. Kriener, K. Segawa, K. Yada, Y. Tanaka, M. Sato, and Y. Ando, Phys. Rev. Lett. 107, 217001 (2011).

- ⁵ V. Mourik, K. Zuo, S. M. Frolov, S. R. Plissard, E. P. A. M. Bakkers, and L. P. Kouwenhoven, *Science* **336**, 1003 (2012).
- ⁶ M. T. Deng, C. L. Yu, G. Y. Huang, M. Larsson, P. Caro, and H. Q. Xu, *Nano Letters* **12**, 6414 (2012).
- ⁷ A. Das, Y. Ronen, Y. Most, Y. Oreg, M. Heiblum, and H. Shtrikman, *Nat. Phys.* **8**, 887 (2012).
- ⁸ L. P. Rokhinson, X. Liu, and J. K. Furdyna, *Nat Phys* **8**, 795 (2012).
- ⁹ J. R. Williams, A. J. Bestwick, P. Gallagher, S. S. Hong, Y. Cui, A. S. Bleich, J. G. Analytis, I. R. Fisher, and D. Goldhaber-Gordon, *Phys. Rev. Lett.* **109**, 056803 (2012).
- ¹⁰ H. O. H. Churchill, V. Fatemi, K. Grove-Rasmussen, M. Deng, P. Caroff, H. Q. Xu, and C. M. Marcus, *Phys. Rev. B* **87**, 241401(R) (2013).
- ¹¹ M. Sato and S. Fujimoto, *Phys. Rev. B* **79**, 094504 (2009).
- ¹² R. M. Lutchyn, J. D. Sau, and S. Das Sarma, *Phys. Rev. Lett.* **105**, 077001 (2010); Y. Oreg, G. Refael, and F. v. Oppen, *ibid.* **105**, 177002 (2010).
- ¹³ M.Z. Hasan and C.L. Kane, *Rev. Mod. Phys.* **82**, 3045 (2010).
- ¹⁴ X. Qi and S. Zhang, *Rev. Mod. Phys.* **83**, 1057 (2011).
- ¹⁵ P. Streda and P. Seba, *Phys. Rev. Lett.* **90**, 256601 (2003).
- ¹⁶ C.L. Kane and E.J. Mele, *Phys. Rev. Lett.* **95**, 226801 (2005).
- ¹⁷ K. Sato, D. Loss, and Y. Tserkovnyak, *Phys. Rev. Lett.* **105**, 226401 (2010).
- ¹⁸ J. Klinovaja, M. J. Schmidt, B. Braunecker, and D. Loss, *Phys. Rev. Lett.* **106**, 156809 (2011); J. Klinovaja, S. Gan-gadharaiyah, and D. Loss, *Phys. Rev. Lett.* **108**, 196804 (2012).
- ¹⁹ J. Klinovaja, G. J. Ferreira, and D. Loss, *Phys. Rev. B* **86**, 235416 (2012).
- ²⁰ J. Klinovaja and D. Loss, *Phys. Rev. X* **3**, 011008 (2013).
- ²¹ J. Klinovaja and D. Loss, arXiv:1304.4542.
- ²² B. Braunecker, G. I. Japaridze, J. Klinovaja, and D. Loss, *Phys. Rev. B* **82**, 045127 (2010).
- ²³ J. Klinovaja, P. Stano, and D. Loss, *Phys. Rev. Lett.* **109**, 236801 (2012).
- ²⁴ M. Kjaergaard, K. Wolms, and K. Flensberg, *Phys. Rev. B* **85**, 020503(R) (2012).
- ²⁵ B. Karmakar, D. Venturelli, L. Chirolli, F. Taddei, V. Giovannetti, R. Fazio, S. Roddaro, G. Biasiol, L. Sorba, V. Pellegrini, and F. Beltram, *Phys. Rev. Lett.* **107**, 236804 (2011).
- ²⁶ M. Menzel, Y. Mokrousov, R. Wieser, J. E. Bickel, E. Vedmedenko, S. Bloegel, S. Heinze, K. v. Bergmann, A. Kubetzka, and R. Wiesendanger, *Phys. Rev. Lett.* **108**, 197204 (2012).
- ²⁷ T.-P. Choy, J. M. Edge, A. R. Akhmerov, and C. W. J. Beenakker, *Phys. Rev. B* **84**, 195442 (2011).
- ²⁸ S. Nadj-Perge, I. K. Drozdov, B. A. Bernevig, and A. Yaz-dani, arXiv:1303.6363.
- ²⁹ S. Nakosai, Y. Tanaka, and N. Nagaosa, arXiv:1306.3686.
- ³⁰ M. A. Ruderman and C. Kittel, *Phys. Rev.* **96**, 99 (1954).
- ³¹ T. Kasuya, *Prog. Theor. Phys.* **16**, 45 (1956).
- ³² K. Yosida, *Phys. Rev.* **106**, 893 (1956).
- ³³ B. Braunecker, P. Simon, and D. Loss, *Phys. Rev. B* **80**, 165119 (2009).
- ³⁴ C. P. Scheller, T.-M. Liu, G. Barak, A. Yacoby, L. N. Pfeif-fer, K. W. West, and D. M. Zumbuhl, arXiv:1306.1940.
- ³⁵ T. Meng and D. Loss, *Phys. Rev. B* **87**, 235427 (2013).
- ³⁶ Subbands can arise from direct hopping inside the wire or indirect hopping via the superconductor, or even from coupled Shiba states induced by the magnetic moments^{28,29,37}.
- ³⁷ A. Yazdani, B. A. Jones, C. P. Lutz, M. F. Crommie, and D. M. Eigler, *Science* **275**, 1767 (1997).
- ³⁸ A. A. Abrikosov, *Fundamentals of the Theory of Metals* (North Holland, 1988).
- ³⁹ P. W. Anderson and H. Suhl, *Phys. Rev.* **116**, 898 (2959).
- ⁴⁰ T. Holstein and H. Primakoff, *Phys. Rev.* **58**, 1098 (1940).
- ⁴¹ A. Yazdani *et al.*, unpublished.
- ⁴² J. Klinovaja and D. Loss, *Phys. Rev. B* **86**, 085408 (2012).
- ⁴³ S. Ryu, A. P. Schnyder, A. Furusaki, and A. W. W. Lud-wig, *New J. Phys.* **12**, 065010 (2010).
- ⁴⁴ D. Rainis, L. Trifunovic, J. Klinovaja, and D. Loss, *Phys. Rev. B* **87**, 024515 (2013).
- ⁴⁵ A. A. Zyuzin, D. Rainis, J. Klinovaja, and D. Loss, arXiv:1305.4187.
- ⁴⁶ E. Prada, P. San-Jose, R. Aguado, *Phys. Rev. B* **86**, 180503(R) (2012).
- ⁴⁷ F. Pientka, G. Kells, A. Romito, P. W. Brouwer, and F. v. Oppen, *Phys. Rev. Lett.* **109**, 227006 (2012).
- ⁴⁸ J. Liu, A. C. Potter, K.T. Law, P. A. Lee, *Phys. Rev. Lett.* **109**, 267002 (2012).
- ⁴⁹ D. Bagrets and A. Altland *Phys. Rev. Lett.* **109**, 227005 (2012).
- ⁵⁰ D. I. Pikulin, J. P. Dahlhaus, M. Wimmer, H. Schomerus, C. W. J. Beenakker, *New J. Phys.* **14**, 125011 (2012).
- ⁵¹ J. D. Sau and S. D. Sarma, arXiv:1305.0554.